



Contents

Regular Papers	
Throughput analysis of partial channel information proportional fairness scheduling N. Hamdi 429	Low-voltage low-power CMOS RF low noise amplifier M.K. Satama, A.M. Soliman 478
Optimal all-to-all broadcast in WDM optical networks with breakdown or power-off transceivers J. Liu, H.-J. Ho, S. Lee 433	An asymmetric defected ground structure with elliptical response and its application as a lowpass filter S.K. Parui, S. Das 483
Switched-current port adaptor configurations for realizing wave filters with improved performance to MOS transistors mismatching N. Kontogiannopoulos, C. Psychalinos 442	Array pattern optimization using electromagnetism-like algorithm J.-Y. Zhang, K.-C. Lee 491
Universal current-mode filter with multiple inputs and one output using MOCCII and MO-CCCA W. Chunhua, L. Haiguang, Z. Yan 448	Letters
Broadband bandpass filters using slotted resonators fed by interdigital coupled lines for improved upper stopband performances M. Meeloon, S. Chaimool, P. Akkaraekthalin 454	Universal current-mode biquad filter using dual output current differencing transconductance amplifier D. Prasad, D.R. Bhaskar, A.K. Singh 497
Analysis of spatially distributed FU-FB S-ALOHA in fading channels using TUA A.U.H. Sheikh, S.B. Rasool 464	Joint transceiver vector precoding based on GMD method for MIMO systems F. Liu, L. Jiang, C. He 502
A translinear-based true RMS-to-DC converter using only npn BJTs K. Kaewdang, K. Kumwachara, W. Surakamponorn 472	Mechanically steerable dielectric fluid antenna H. Fayad, P. Record 506
	Joint blind estimation of symbol timing and carrier frequency offset for 2×2 MIMO-OFDM system based on cyclostationarity Y. Niu, Y. Shen 513
	High-order mixed-mode OTA-C universal filter C.-N. Lee, C.-M. Chang 517

◆ www.elsevier.de/aeue

ISSN 1434-8411
Int. J. Electron. Commun. (AEU)
63(2009)6 · pp. 429-522

6/2009
Volume 63

This article appeared in a journal published by Elsevier. The attached copy is furnished to the author for internal non-commercial research and education use, including for instruction at the authors institution and sharing with colleagues.

Other uses, including reproduction and distribution, or selling or licensing copies, or posting to personal, institutional or third party websites are prohibited.

In most cases authors are permitted to post their version of the article (e.g. in Word or Tex form) to their personal website or institutional repository. Authors requiring further information regarding Elsevier's archiving and manuscript policies are encouraged to visit:

<http://www.elsevier.com/copyright>



Low-voltage low-power CMOS RF low noise amplifier

Mohammed K. Salama*, Ahmed M. Soliman

Department of Electronics and Communication, Cairo University, Giza, Egypt

Received 28 January 2008; accepted 30 March 2008

Abstract

In this paper, a 1 V, 2 GHz CMOS low-noise amplifier (LNA) was developed intended for use in the front-end receiver. The circuit is simulated in standard 0.25 μm CMOS MOSIS. The LNA gain is 25.675 dB, noise figure (NF) is 4 dB, reverse isolation (S_{12}) is -134.3 dB, input return loss (S_{11}) is -14.6 dB, output return loss (S_{22}) is -13.34 dB, and the power consumption is 5.13 mA from a single 1 V power supply. One of the features of the proposed design is using a three-component cascode limitation, one of it is a transistor, to reduce the supply voltage.

© 2008 Elsevier GmbH. All rights reserved.

Keywords: Low-noise amplifier; RF front-end; Global system for mobile communication (GSM); Global positioning system (GPS); Wireless local area network (WLAN)

1. Introduction

As wireless product such as cellular phones, global system for mobile communication (GSM), global positioning satellite (GPS), wireless local area network (WLAN), etc. became an everyday part of people's lives, the need for higher performance at low costs and low-power consumption became even more important in addition to the size of the wireless device. One of the important blocks in the receiver is the low-noise amplifier (LNA). Today the present goal is to reduce the power consumption, which leads to an increase of the battery-use time and of cost as well [1]; one of the ways of achieving this is to reduce the supply voltage [2].

In this paper, a modified cascode LNA is presented. Noise figure (NF) is an important parameter for RF LNA design; NF is a measure of how much the signal-to-noise ratio (SNR) degrades as the signal passes through a system [3]. The NF simulation is presented in Section 2.4. Recent research in the

design of LNAs has focused on the NF analysis and noise optimization in addition to impedance matching as presented in detail in [3,5–17,19–21].

2. LNA design

LNA is the first block in wireless receivers. It is responsible for providing reasonable power gain and linearity, while not degrading the SNR. In the design of LNAs, there are several common goals; these include minimizing the NF of the amplifier, providing gain with sufficient linearity, and providing a stable $50\ \Omega$ input impedance to terminate an unknown length of transmission line, which delivers signal from the antenna to the amplifier [4].

Fig. 1 is the most popular narrow-band LNA. It is narrow-band because impedance matching is only established within a very narrow frequency range due to the resonant nature of the reactive matching network. Impedance matching is established by inductive degeneration. Around the operation frequency $\omega_o = 1/\sqrt{C_{gs}(L_g + L_s)}$, the input impedance only presents a real part $Z_{in} = g_m/C_{gs}L_s$; detailed analysis

* Corresponding author.

E-mail addresses: Mksalama@link.net (M.K. Salama), asoliman@idsc.net.eg (A.M. Soliman).

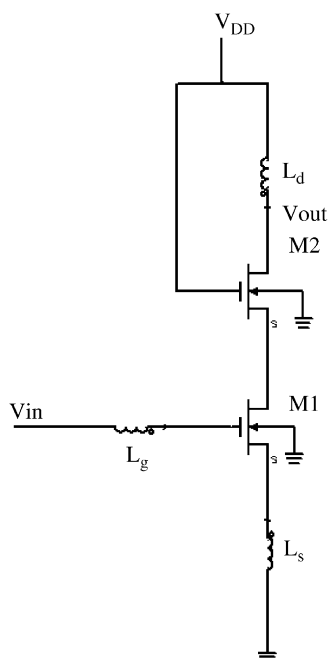


Fig. 1. Shaeffer and Lee low noise amplifier [5].

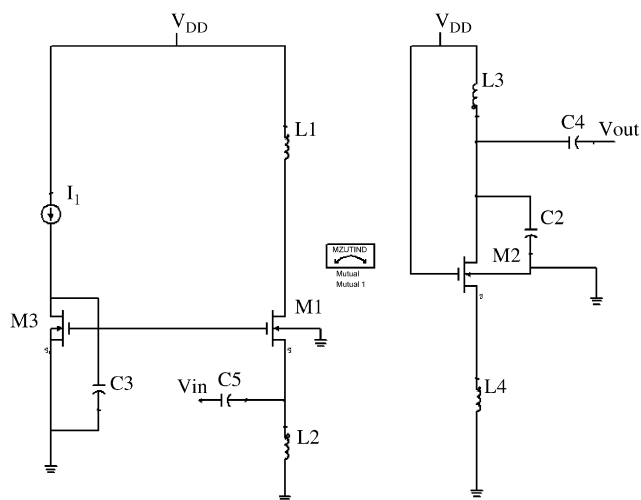


Fig. 2. Modified cascade low-noise amplifier.

is found in [5]. The high-output impedance is an important property of the cascode structure [19]. To reduce the cascode number of elements, the mutual inductance properties between two inductors were used as shown in Fig. 2, L_1 is connected to the drain of M_1 and L_4 to the source of M_2 in Fig. 1 and the signal is transferred from the drain of M_1 to the source of M_2 through the mutual inductance between L_1 and L_4 . As shown in Fig. 2, the LNA differs by one additional capacitor C_2 compared to the typical cascode LNA. The insertion of this capacitance adds a degree of freedom to play with the noise performance in addition to the gain at low-power consumption.

Also the input is applied on the M_1 source instead of the M_1 gate, which makes the body effect increase the equivalent transconductance of the stage [19], as shown in the next subsection.

2.1. Amplifier's gain analysis

The voltage transfer function of the proposed circuit can be written as follows:

$$A_v = (1 + r_{o1}(g_{m1} + g_{mb1}))(1 + r_{o2}(g_{m2} + g_{mb2})) * \frac{S^3 M_1 L_1 L_2}{\sum_{n=0}^8 \delta_n s^n} \quad (1)$$

where

$$\delta_n = L_2 \beta_{n-1} - R_1 \alpha_n - r_{o2} \beta_n - R_1 L_2 C_2 \alpha_{n-2} - r_{o2} L_2 C_2 \beta_{n-2} \quad (2)$$

for $n = 0-8$,

$$\alpha_6 = \alpha_7 = \alpha_8 = 0,$$

$$\beta_7 = \beta_8 = 0,$$

$$\alpha_t = 0 \text{ and } \beta_t = 0 \text{ for } t < 0$$

g_{m1} and g_{m2} are the transconductance of M_1 and M_2 , respectively, and g_{mb1} , g_{mb2} are the body-effect transconductance of M_1 and M_2 , respectively. C_{gs1} and C_{gs2} , are the gate-source capacitance of M_1 and M_2 , respectively. C_{db1} and C_{db2} are the drain-body depletion capacitance of M_1 and M_2 , respectively. C_{gd1} and C_{gd2} are the gate-drain capacitance of M_1 and M_2 , respectively. C_{sb1} and C_{sb2} are the source-body depletion capacitance of M_1 and M_2 [18]. R_1 , R_2 , R_3 , and R_4 are the loss resistance in series with the inductance L_1 , L_2 , L_3 , and L_4 , respectively. β_t and α_t are the functions of M_1 and M_2 device parameters as shown in Appendix A. As seen from Eq. (1), the mutual inductance M_1 between L_1 and L_4 helps in giving extra freedom for controlling the conversion gain taking into account the layout fabrication limitation. Also the body effect affects positively the LNA conversion gain.

Eq. (2) shows that the insertion of the capacitor C_2 gives another degree of freedom to control the LNA conversion gain.

2.2. S-parameters simulation result

The circuit of Fig. 2 is simulated with ADS simulation tools. Fig. 3 shows the input return loss simulation result (-14.6 dB at resonance frequency 2 GHz).

The reverse isolation result of the LNA is -134.3 dB at 2 GHz. The LNA gain and the output return loss are presented in Fig. 3. The gain of the LNA at the operating frequency is 25.675 dB and the S_{22} is -13.34 dB.

2.3. Amplifier stability

Another important consideration in the LNA design is the amplifier stability. The conditions for unconditionally stable in terms of S -parameters [21] are:

$$|\Delta| = |S_{11}S_{22} - S_{12}S_{21}| > 1 \quad (3)$$

and

$$K = \frac{1 - |S_{11}|^2 - |S_{22}|^2 + |S_{11}S_{22} - S_{12}S_{21}|^2}{2|S_{12}S_{21}|} < 1 \quad (4)$$

From the above equation, the presented LNA is stable at the frequency of interest 2 GHz as presented in Fig. 4. The presented LNA is stable over a wide frequency range (unconditionally stable). A wide frequency range (0.5–4 GHz) was considered an order to make sure that none of the out-of-the-band frequencies can cause the LNA to oscillate.

2.4. Noise performance simulation result

The NF of the presented LNA is 4 dB at frequency 2 GHz as presented in Fig. 5. NF is affected negatively by the degeneration inductor loss resistance in the transistor M_1 source.

2.5. Power consumption

Today the present goal is to reduce the power consumption, which leads to the increase in the battery-use time and

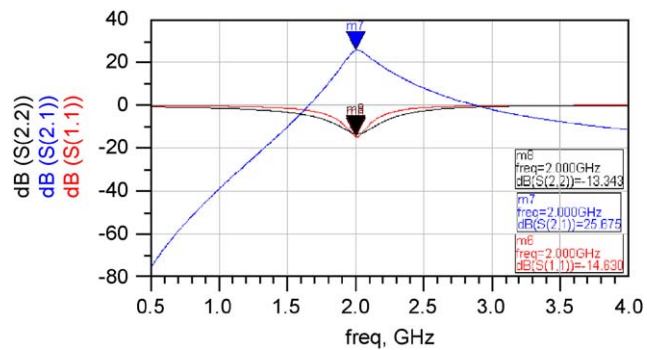


Fig. 3. Input return loss, gain, and output return loss of the LNA.

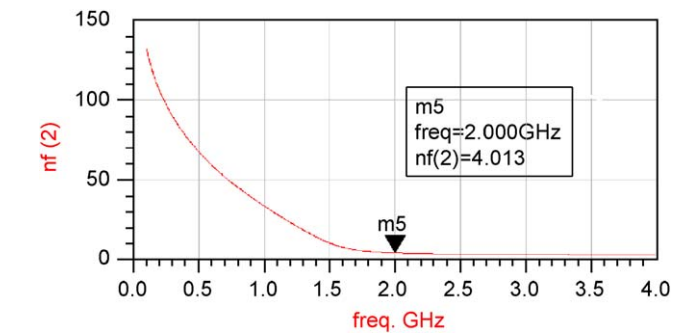
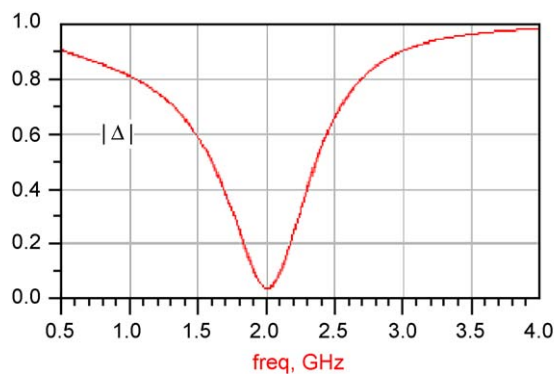


Fig. 5. Noise figure.

of the cost as well. The power consumption reduction is one of the requirements today; one of the ways achieving this is to reduce the supply voltage. In the presented design, the three element limitation including one transistor per stage is used to reduce the supply voltage to 1 V or less, which leads to reducing the power consumption and using a battery for a long time. The power consumption of the presented LNA is 5.13 mA from a 1 V single supply.

3. Conclusion

A low-voltage CMOS LNA based on a modification done to the traditional cascode LNA was presented. Using cascode elements of the reduction technique based on the two transistors limitation to reduce the supply voltage that leads to increase the battery life time on most applications. The input signal is inserted in the M_1 source to take the advantage of the body effect to help increase the conversion gain. The insertion of the capacitor C_2 gives another degree of freedom to control the LNA gain. The LNA is simulated in standard 0.25 μm . The LNA presented here is useful in RF signal-processing applications, in the front-end transceiver, WLAN, and ISM.

The circuit presented here is compared with other circuits in terms of performance and the results are summarized in Table 1.

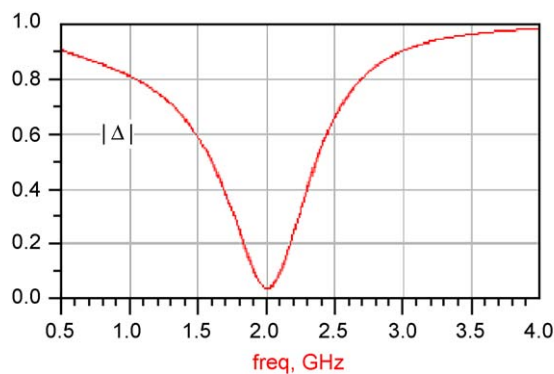


Fig. 4. Stability condition (5) and stability factor K .

Table 1. Comparison of LNA performances

Ref.	S_{11} (dB)	Gain (dB)	NF (dB)	Freq. (MHz)	Supply voltage (V)	Tech. (CMOS) (μm)
[5]	–	22	3.5	1000	1.5	0.6
[4]	–	19.7	2.37	1900	2.25	0.2
[12]	–14	12.74	2.5	2100	3.5	0.5
[22]	–	14.9	3	2200	1.2	0.25
[23]	–19.7	18	1.6	2000	1.6	0.13
[24]	–11.5	11	2.95	900	2.5	0.35
[25]	–8	14.5	2.6	2000	1.5	0.13
This design	–14.6	25.67	4	2000	1	0.25

Appendix A

$$A_v = (1 + r_{o1}(g_{m1} + g_{mb1}))(1 + r_{o2}(g_{m2} + g_{mb2}))$$

$$* \frac{S^3 M_1 L_1 L_2}{\sum_{n=0}^{n=8} \delta_n s^n}$$

where

$$\delta_n = L_2 \beta_{n-1} - R_1 \alpha_n - r_{o2} \beta_n - R_1 L_2 C_2 \alpha_{n-2}$$

$$- r_{o2} L_2 C_2 \beta_{n-2}$$

for $n = 0-8$

$$\alpha_t = 0 \text{ and } \beta_t = 0 \text{ for } t < 0$$

$$\alpha_t = F_1(r_{o1}, r_{o2}, R_3, R_4, R_s, L_1, L_2, L_3, L_4, M_1, C_1,$$

$$C_{gs1}, C_{db1}, C_{gd1}, g_{m1}, g_{mb1}, g_{m2}, g_{mb2})$$

where

$$\alpha_0 = R_4(R_3 + r_{o1})$$

$$\alpha_1 = R_3 L_1 A_1 + \frac{L_1}{R_s}(r_{o1} R_4 + R_3 R_4)$$

$$+ r_{o1}(L_4 + R_3 R_4(C_{db1} + C_{gd1}))$$

$$+ R_3 L_4 + R_4 L_3$$

$$\alpha_2 = L_1 A_1(L_4 + R_3 R_4(C_{db1} + C_{gd1})) + (r_{o1} R_4$$

$$+ R_3 R_4) L_1 C_1 + r_{o1}(R_3 L_4 + R_4 L_3)(C_{db1} + C_{gd1})$$

$$+ (L_3 L_4 - M_1^2) + \frac{L_1}{R_s}(r_{o1}(L_4 + R_3 R_4(C_{db1} + C_{gd1}))$$

$$+ R_3 L_4 + R_4 L_3)$$

$$\alpha_3 = L_1 A_1(C_{db1} + C_{gd1})(R_3 R_4 + R_4(L_3 - M_1))$$

$$+ r_{o1}(C_{db1} + C_{gd1})(L_3 L_4 - M_1^2)$$

$$+ \frac{L_1}{R_s}(r_{o1}(R_3 L_4 + R_4 L_3)(C_{db1} + C_{gd1})$$

$$+ (L_3 L_4 - M_1^2)) + L_1 C_1(r_{o1}(L_4 + R_3 R_4(C_{db1} + C_{gd1}))$$

$$+ R_3 L_4 + R_4 L_3)$$

$$\alpha_4 = \left(L_1 A_1 + \frac{L_1}{R_s} r_{o1} \right) (C_{db1} + C_{gd1})(L_3 L_4 - M_1^2)$$

$$+ L_1 C_1(r_{o1}(R_3 L_4 + R_4 L_3)(C_{db1} + C_{gd1})$$

$$+ (L_3 L_4 - M_1^2))$$

$$\alpha_5 = r_{o1} L_1 C_1 (C_{db1} + C_{gd1})(L_3 L_4 - M_1^2)$$

$$\alpha_6 = \alpha_7 = \alpha_8 = 0$$

and

$$\beta_t = F_2(r_{o1}, r_{o2}, R_3, R_4, R_s, L_1, L_2, L_3, L_4, M_1, C_1,$$

$$C_{gs1}, C_{gs2}, C_{sb2}, C_{db1}, C_{gd1}, g_{m1}, g_{mb1}, g_{m2}, g_{mb2})$$

where

$$\beta_0 = R_1(R_3 + r_{o1})$$

$$\beta_1 = L_1 R_3 + r_{o1} R_1 R_3 (C_{db1} + C_{gd1}) + R_1 (L_3 + R_3 R_4 (C_{gs2}$$

$$+ C_{sb2})) + A_1 L_1 + r_{o1} L_1 + r_{o1} R_1 R_4 (C_{gs2} + C_{sb2})$$

$$\beta_2 = R_3 (L_1 C_1 R_1 + L_1 (A_1 + r_{o1})(C_{db1} + C_{gd1})) + (L_3$$

$$+ R_3 R_4 (C_{gs2} + C_{sb2}))(L_1 + r_{o1} R_1 (C_{db1} + C_{gd1}))$$

$$+ R_1 (C_{gs2} + C_{sb2})(R_3 L_4 + R_4 L_3) + r_{o1} R_1 L_1 C_1$$

$$+ R_4 (C_{gs2} + C_{sb2})(A_1 + r_{o1}) L_1$$

$$+ r_{o1} R_1 R_4 (C_{gs2} + C_{sb2})$$

$$\beta_4 = (L_3 + R_3 R_4 (C_{gs2} + C_{sb2}))(r_{o1} R_1 L_1 C_1 (C_{db1} + C_{gd1}))$$

$$+ (C_{gs2} + C_{sb2})(R_3 L_4 + R_4 L_3)(R_1 L_1 C_1$$

$$+ (A_1 + r_{o1})(C_{db1} + C_{gd1}) L_1)$$

$$+ (L_3 L_4 - M_1^2)(L_1 + r_{o1} R_1 (C_{db1} + C_{gd1}))$$

$$+ r_{o1} R_1 L_1 L_4 C_1 (C_{gs2} + C_{sb2})$$

$$\beta_3 = R_3 (r_{o1} R_1 L_1 C_1 (C_{db1} + C_{gd1}) + (L_3 + R_3 R_4 (C_{gs2}$$

$$+ C_{sb2}))(R_1 L_1 C_1 + (A_1 + r_{o1})(C_{db1} + C_{gd1}) L_1)$$

$$+ (C_{gs2} + C_{sb2})(R_3 L_4 + R_4 L_3)(L_1 + r_{o1} R_1 (C_{db1}$$

$$+ C_{gd1})) + R_1 (L_3 L_4 - M_1^2) + r_{o1} R_1 L_1 C_1 R_4 (C_{gs2} + C_{sb2})$$

$$+ L_4 (C_{gs2} + C_{sb2})(A_1 + r_{o1}) L_1$$

$$\beta_5 = (C_{gs2} + C_{sb2})(R_3 L_4 + R_4 L_3)(r_{o1} R_1 L_1 C_1 (C_{db1} + C_{gd1}))$$

$$+ (L_3 L_4 - M_1^2)(R_1 L_1 C_1 + (A_1 + r_{o1}) L_1 (C_{db1} + C_{gd1}))$$

$$\beta_6 = (L_3 L_4 - M_1^2)(r_{o1} R_1 L_1 C_1 (C_{db1} + C_{gd1}))$$

$$\beta_7 = \beta_8 = 0$$

References

- [1] Behzad R. Challenges in portable RF transceiver design. IEEE J Circuits Devices 1996;12:27.

- [2] Salama MK, Soliman AM. Low-voltage low-power CMOS RF four-quadrant multiplier. *AEU-Int J Electron Commun* 2003;57:74–8.
- [3] Behzad R. *RF microelectronics*. Upper Saddle River, NJ: Prentice-Hall; 1998.
- [4] Ny JL, Thudi B, McKenna J. A 1.9 GHz low noise amplifier. *EECS 522 Analog Integrated Circuit Project*, Winter 2002; 1–6.
- [5] Shaeffer DK, Lee TH. A 1.5 V, 1.5 GHz CMOS low noise amplifier. *IEEE J Solid-State Circuits* 1997;32:745–59.
- [6] Allstot DJ, Li X, Shekhar S. Design considerations for CMOS low-noise amplifiers. *IEEE Radio Freq Integrated Circuits Symp* 2004; 97–100.
- [7] Park S, Kim W. Design of A 1.8 GHz low-noise amplifier for RF front-end in a 0.8 μ m CMOS technology. *IEEE Trans Consum Electron* 2001; 47.
- [8] Andreani P, Sjöland H. Noise optimization of an inductively degenerated CMOS low noise amplifier. *IEEE Trans Circuits Syst-II: Analog Digital Signal Process* 2001;48:835–41.
- [9] Manku T. Microwave CMOS-device physics and design. *IEEE J Solid-State Circuits* 1999;34:277–85.
- [10] Behbahani F, Leete JC, Kishigami Y, Roithmeier A, Hoshino K, Abidi A. A 2.4-GHz low-IF receiver for wideband WLAN in 0.6- μ m CMOS-architecture and front-end. *IEEE J Solid-State Circuits* 2000; 35.
- [11] Ny JL, Thudi B, McKenna J. A 1.9 GHz low noise amplifier. *EECS 522 Analog Integrated Circuit Project*, Winter 2002; 1–6.
- [12] Govind V, Dalmia S, Swaminathan M. Design of integrated low noise amplifiers (LNA) using embedded passives in organic substrates. *IEEE Trans Adv Packag* 2004;27:79–89.
- [13] Nguyen T, Oh N, Cha C, Oh Y, Ihm G, Lee S. Image-rejection CMOS low-noise amplifier design optimization techniques. *IEEE Trans Microwave Theory Tech* 2005;53:538–46.
- [14] Zhuo W, Li X, Shekhar S, Embabi SHK, Pineda de Gyvez J, Allstot DJ, Sanchez-Sinencio E. A capacitor cross-coupled common-gate low-noise amplifier. *IEEE Trans Circuits Syst-II: Express Briefs* 2005;52:875–9.
- [15] Sun K, Tsai Z, Lin K, Wang H. A noise optimization formulation for CMOS low-noise amplifiers with on-chip low-Q inductors. *IEEE Trans Microwave Theory Tech* 2006;54:1554–60.
- [16] Belostotski L, Haslett JW. Noise figure optimization of inductively degenerated CMOS LNAs with integrated gate inductors. *IEEE Trans Circuits Syst-I* 2006;53:1409–22.
- [17] Lu Y, Yeo KS, Cabuk A, Ma J, Do MA, Lu Z. A novel CMOS low-noise amplifier design for 3.1 to 10.6-GHz ultra-wideband wireless receivers. *IEEE Trans Circuits Syst-I: Regular Papers* 2006;53:1684–92.
- [18] Gray PR, Meyer RG. *Analysis and design of analog integrated circuits*. 3rd ed., New York: Wiley; 1993.
- [19] Behzad R. *Design of analog CMOS integrated circuits*. New York: McGraw-Hill; 2001.
- [20] Lee TH. *The design of CMOS radio frequency integrated circuits*. New York: Cambridge University Press; 2000.
- [21] Gonzalez G. *Microwave transistor amplifiers: analysis and design*. 2nd ed., Upper Saddle River, NJ: Prentice-Hall; 1997.
- [22] Youn YS., Chang JH, Koh KJ, Lee YJ, Yu HK. A 2 GHz 16 dBm IIP3 low noise amplifier in 0.25 μ m CMOS technology. In: *IEEE International Solid-State Circuits Conference*, San Francisco, CA; February 2003. p. 452–3.
- [23] Sivonen P, Pärssinen A. Analysis and optimization of packaged inductively degenerated common-source low-noise amplifiers with ESD protection. *IEEE Trans Microwave Theory Tech* 2005;53:1304–13.
- [24] Ganesan S, Sánchez-Sinencio E, Silva-Martinez J. A highly linear low-noise amplifier. *IEEE Trans Microwave Theory Tech* 2006;54:4079–85.
- [25] Wei-Hung C, Gang L, Boos Z, Ali MN. A highly linear broadband CMOS LNA employing noise and distortion cancellation. *IEEE Radio Frequency Integrated Circuits Symp* 2007; 61–4.



Mohammed Khalaf Salama received his B.Sc. (with honors) degree and his M.S. degree in electrical engineering from Cairo University, Giza, Egypt, in 1998 and 2003, respectively. He is currently working for his Ph.D. degree in electrical engineering at Cairo University, Giza, Egypt. His research interests include RF integrated circuit and low-voltage low-power RF Front-end design for GSM, GPS, ISM, and Wireless LAN applications “IEEE802.11 standards WLAN applications”.



Ahmed Mohamed Soliman received his B.Sc. degree with honors from Cairo University, Giza, Egypt, in 1964, his M.S. and Ph.D. degrees from the University of Pittsburgh, Pittsburgh, PA, USA, in 1967 and 1970, respectively, all in Electrical Engineering. He is currently Professor Electronics and Communications Engineering Department, Cairo University, Egypt. From

September 1997 to September 2003, Dr. Soliman served as Professor and Chairman Electronics and Communications Engineering Department, Cairo University, Egypt. He has held visiting academic appointments at San Francisco State University, Florida Atlantic University and the American University in Cairo. In 1977, Dr. Soliman was honoured with the First Class Science Medal, from the President of Egypt, for his services in the field of Engineering and Engineering Education. He is a Member of the Editorial Board of the *IET Circuits, Devices and Systems*. He is a Member of the Editorial Board of *Analog Integrated Circuits and Signal Processing*. He also served as Associate Editor of the *IEEE Transactions on Circuits and Systems I (Analog Circuits and Filters)* from December 2001 to December 2003 and is Associate Editor of the *Journal of Circuits, Systems and Signal Processing* since January 2004.